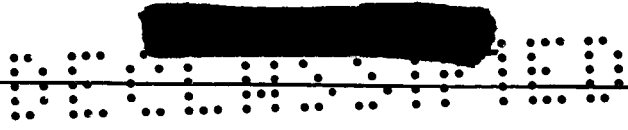


NACA RM L5  
2a



# NACA

Declassified by authority of NASA  
Classification Change Notices No. 213  
Dated \*\* 6-30-71

## RESEARCH MEMORANDUM

STABILITY OF BALLISTIC REENTRY BODIES

By

John D. Bird

Langley Aeronautical Laboratory  
Langley Field, Va.

and

David E. Reese, Jr.

Ames Aeronautical Laboratory  
Moffett Field, Calif.

CASE  
COPY  
FILE

CLASSIFICATION CODE  
UNCLASSIFIED

TO \_\_\_\_\_

By Authority of TD-70-180 Date 1 MAR 1971

### NATIONAL ADVISORY COMMITTEE FOR AERONAUTICS

WASHINGTON  
August 11, 1958



## RESEARCH MEMORANDUM

## STABILITY OF BALLISTIC REENTRY BODIES\*

By John D. Bird and David E. Reese, Jr.

## SUMMARY

Various features of the stability of ballistic reentry shapes are discussed, including those considerations pertinent to ballistic-missile and manned-satellite reentry capsules. Calculations and aerodynamic data are used to indicate the problems involved. It is concluded that, with proper allowance for desirable geometrical features, the attainment of satisfactory stability of reentry bodies having subsonic terminal velocities is not too difficult but, in efforts to minimize weight in solution of the heating problem, undesirable features may be introduced which will cause marginal stability characteristics. The attainment of satisfactory stability of reentry bodies having supersonic terminal velocities appears to offer fewer problems.

## INTRODUCTION

The analysis of Allen (ref. 1) indicated the essential features of the problem of reentry stability in terms of Bessel functions. In this work and the related work of others, the powerful constraining effect on the motion of the rapid increase of dynamic pressure was shown in addition to the destabilizing influence of the drag force. The criterion of stability was expressed by Allen in reference 1 in terms of a now well-known damping factor which includes the drag, lift, and pitch-damping coefficients. This solution is good for the range of Mach numbers where the stability derivatives are essentially constant as assumed in the analysis and only undergoes some modification near and below the transonic region where the aerodynamic characteristics change radically and the motion has slowed to the point where the influence of gravity becomes significant. In this work it was shown that satisfactory directional stability was the factor of primary concern down to an altitude in the vicinity of 100,000 feet for the densities of missiles generally under consideration and that the

---

\*Title, Unclassified.



damping derivatives, that is, the drag, lift-curve slope, and the damping in pitch, made themselves felt primarily below that altitude.

The purpose of the present investigation is, first, to discuss some aerodynamic characteristics of blunt reentry shapes and to give some indication of the significance of these characteristics as related to the dynamics of ballistic-missile reentry bodies, second, to discuss the dynamics of a manned lightweight reentry capsule and, third, to mention a few points in connection with work on slender, high-terminal-velocity bodies for ballistic missiles.

#### SYMBOLS

|                                    |   |
|------------------------------------|---|
| $C_D$                              | drag coefficient  |
| $C_{L\alpha}$                      | lift-coefficient derivative with respect to angle of attack, per radian   |
| $C_{m\dot{q}} + C_{m\dot{\alpha}}$ | pitch-damping derivative based on $\frac{l}{2V}$  |
| $l$                                | characteristic length, generally maximum diameter   |
| $\sigma$                           | radius of gyration  |
| $M$                                | Mach number   |
| $\alpha$                           | angle of attack   |
| $\alpha_E$                         | angle of attack on reentry to atmosphere  |
| $W$                                | weight of reentry body  |
| $A$                                | reference area, generally maximum cross-sectional area  |
| $C_{N\alpha}$                      | normal-force derivative with respect to angle of attack, per radian   |
| $I_Y$                              | moment of inertia   |
| $\gamma$                           | flight-path angle, positive up  |
| $C_{m\alpha}$                      | pitching-moment-coefficient derivative with respect to angle of attack, nondimensionalized by reference area and length, per radian |
| $V$                                | forward velocity  |



  
SECRET

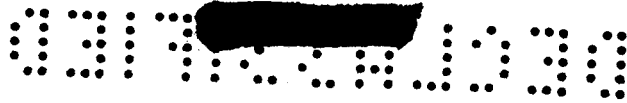
R Reynolds number  
f frequency  
 $q_{max}$  maximum dynamic pressure  
t time

## DISCUSSION

Examples of the pitch damping obtained for blunt shapes at various Mach numbers are shown in figures 1 and 2. The data shown in these figures in the subsonic Mach number range were obtained in the Ames 12-foot pressure tunnel by Donald A. Buell, whereas those in the supersonic Mach number range were obtained in the Ames 8- by 7-foot Unitary Plan wind tunnel by Benjamin H. Beam. Figure 1 shows results obtained on a very shallow reentry shape. It can be seen that unstable pitch damping is obtained in the supersonic region for this shape with a moderately sized afterbody. This would result in an undesirable dynamic behavior of this configuration unless there is an appreciable modification of the pitch damping in the lower or higher supersonic Mach number range. One of the most interesting points in connection with these data is the influence of afterbody shape. At the supersonic Mach numbers increasing the size of the afterbody was beneficial (made the pitch damping more negative), whereas at both subsonic and supersonic speeds reducing the size of the afterbody was beneficial. This beneficial effect of afterbody-size reduction at subsonic speeds is better shown by the data of figure 2 which are for a parabolic configuration. For this configuration, reduction of afterbody size produced a pronounced effect at subsonic speeds but had essentially no effect at the supersonic speeds. Also, the pitch damping for this configuration was stable in the supersonic region as contrasted with the results for the more shallow configuration of figure 1.

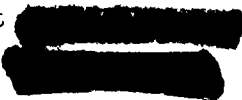
A factor that has been given some attention in connection with damping measurement is that of the influence of a small angle of attack that may arise from unsymmetrical distortion of the body. In the case of the blunt shallow reentry shapes this effect has been found to be quite significant at a Mach number of 2.5. (See fig. 3.) Small angles of attack are sufficient to cause marked changes in the pitch damping. In the case of the configuration with a moderate afterbody the damping is changed from an unstable value to a stable one by a change of  $2^\circ$  in angle of attack. Damping of the configuration with a small afterbody,





however, becomes unstable at about  $1^\circ$  angle of attack. These results show a decided nonlinear damping behavior which dictates the study of pitch damping to amplitudes commensurate with those to be tolerated in the particular application in order to obtain a reasonable perspective. The results shown in figure 3 indicate the strong probability of limit cycle operation for the model with the moderate-sized afterbody.

The effect of a change in pitch damping on reentry body motion is shown in figure 4. Calculations are shown in this figure for optimum-range intercontinental-ballistic-missile (ICBM) reentry conditions for which the aerodynamic derivatives used are given in table I. These calculations were made by use of an IBM type 704 electronic data processing machine. The complete nonlinear equations of motion were employed. In one case in figure 4 the aerodynamic characteristics correspond generally to those of the shallow body with moderately sized afterbody, and in the other case the aerodynamic characteristics correspond generally to those of the shallow body with a small afterbody. It can readily be seen that an increase of damping is beneficial. The calculation diverges to considerably greater amplitude prior to a Mach number of 1 for negative pitch damping than for zero pitch damping. When the stable subsonic pitch damping comes into play, the motion of the body with small afterbody subsides. The calculation with negative pitch damping was not carried completely to the ground. It should be remembered that limit cycle performance will very probably prevent bodies similar to the shallow model with moderately sized afterbody from exceeding a certain relatively small amplitude. In general, considerable divergence can be tolerated prior to a Mach number of 1.0 if good subsonic damping is present and care is taken not to have too great an angle of attack at reentry. Pitch damping as great as  $-0.3$  would give an almost linear decay of the pitching motion to zero amplitude at about an altitude of 40,000 feet. Artificial pitch damping as great as  $-3.0$  would cause the motion to subside by the time an altitude of 100,000 feet is reached.

One possibility for improving the stability characteristics of subsonic reentry bodies in the transonic region that has been given some thought involves the use of a spool-like form as shown in figures 5 and 6. These data were obtained in the Langley transonic blowdown tunnel and Mach 3 jet by Lewis R. Fisher and William Letko, respectively. The theory behind the use of this configuration is that the flare at the end of the body will be extremely effective in the near transonic region and, hence, will contribute to the pitch damping in large measure at low speeds but will not greatly affect the aerodynamic characteristics nor will the flare encounter great heating loads at the higher speeds, because of its location, if it is made sufficiently small. Some beneficial effect should be obtained for this arrangement at the extremely high reentry altitudes because of the improvements in directional stability at the large angles of attack that may be encountered without precise orientation by automatic means. It  at a surprisingly large value

of directional stability is obtained with this arrangement in comparison with that obtained with the simple flared model at the left in figure 5. Results at a Mach number of 3.0 on somewhat different models indicate that spool models do not experience as great an increase of stability over simple flared models for supersonic speeds as was the case for transonic speeds (fig. 6). The damping in pitch of a spool model can be seen from the data of figure 7. These data were obtained in the Langley high-speed 7- by 10-foot tunnel by Herman S. Fletcher. The simple flared model shows unstable damping at the higher subsonic speeds, whereas the spool model shows a powerful damping influence. It is quite likely that an optimum spool shape would have less flare than the models for which data are shown because these models have more directional stability than is required.

The unstable pitch damping shown for the simple flared model as the transonic region is approached has been obtained for other shapes in greater or lesser degree and has caused some concern. However, a considerable degree of unstable damping may be tolerated in the transonic region for subsonic-terminal-velocity bodies which make rapid transit of the transonic region if the subsonic pitch damping is stable. This unfavorable pitch damping effect can be seen from the calculations shown in figure 8, the conditions for which are given in table I. It can be seen in figure 8 that a reversal in sign of the pitch damping in the transonic region does not impose an intolerable burden because not too great an amplitude is reached before the transonic region is passed. The result may be entirely different, of course, for a reentry body having a transonic terminal velocity; this body would be exposed to any transonic peculiarity for a much longer period of time.

Recently there has been a general belief that a high-drag bluff body would make an adequate minimum reentry body for a man-carrying satellite (ref. 2). In such an application a low angle of reentry would be employed in order to minimize the acceleration on the occupant. An example of the motion of a vehicle on reentry to the atmosphere is shown in figure 9. Aerodynamic data for the reentry capsule shown in this figure were used for the present calculation. The various mass and aerodynamic quantities used in the calculation are given in table I. The equations for these calculations included the effect of the earth's curvature and were integrated by use of an IBM type 704 electronic data processing machine. The sketch in figure 9 shows the general character of this reentry. A maximum deceleration of 9.9g is encountered at an altitude of 145,000 feet. Also shown in this figure is a plot of the amplitude envelope of the oscillation during reentry for an assumed error in alinement with the flight path of  $1^\circ$  at reentry. The first few cycles of the oscillation are shown as a dashed line in the right-hand side of this plot. The amplitude of oscillation at Mach number 1 is much the same as that at reentry. Thereafter, an increase in

divergence occurs in spite of the stable subsonic pitch damping. The damping factor is unstable in this region as well as for the remainder of the reentry because of the negative lift-curve slope. An increase of pitch damping in the subsonic region to  $-0.20$  effected by adding a tail assembly or flare produces a more stable behavior. The frequency history of the capsule during reentry is presented in figure 10. It is evident from the figure that the frequency and dynamic pressure are not excessive. The maximum frequency is about 1.0 cycle per second which occurs at an altitude of 145,000 feet. The maximum normal acceleration, which is extremely low because of the small normal lift-curve slope and small error in alinement of the satellite on reentry, is about  $0.12g$  and occurs at an altitude of about 125,000 feet. These results indicate this to be a reasonable form of reentry vehicle from the stability point of view.

An example of the negative lift-curve slopes of several forms of blunt reentry bodies which contribute to the low-altitude divergence shown for the satellite is given in figure 11. These data were obtained in the Langley transonic blowdown tunnel by Lewis R. Fisher and Joseph R. DiCamillo. In this figure the lift-curve and pitching-moment-curve slopes are shown for several blunt shapes at a Mach number of 1.0. It can be seen that the very blunt forms have destabilizing negative lift-curve slopes and that there is a pronounced Reynolds number effect for one of the intermediate shapes. The negative lift-curve slopes for the blunt rounded-corner forms shown in figure 11 become somewhat smaller as the supersonic region is entered and the aerodynamics approaches the Newtonian consideration more closely. Instability from this particular source may be well in evidence in the terminal phase of flight for bodies with relatively low pitch damping.

Recently, it has become apparent that, for ballistic missiles, terminal velocities to a Mach number of 2.0 or higher are not unreasonable with present methods and materials. As a result, increased emphasis has been given to long slender shapes having low rather than high drag coefficients. An examination of the Allen damping factor (ref. 1)

$$C_D - C_{L\alpha} + \frac{1}{2}(C_{m\dot{q}} + C_{m\dot{\alpha}})\left(\frac{1}{\sigma}\right)^2$$

indicates that this trend is favorable inasmuch as the destabilizing drag quantity is reduced considerably when long slender shapes are used. In addition, the sometimes troublesome transonic region is avoided completely, and the possibility of destabilizing negative lift-curve slopes is eliminated because the lift-curve slope of slender, more pointed bodies is positive.

One approach to the design of ballistic missiles having high terminal velocities might be to utilize slender arrangements in the form of artillery shells that have no stabilizing surfaces to protect from heating. Such an arrangement would generally have some degree of instability if packaged more or less uniformly which would have to be counteracted by sufficient spin or by other means to provide stabilization. An examination of the spin stability criterion indicates that the required spin rates are likely to be excessive for so complicated a device as a reentry warhead or a man-carrying satellite. Also, the higher gyroscopic stiffness introduced tends to maintain large amplitudes of yaw well into the region of high heating. Such behavior may be advantageous for applications in which appreciable loss of heat by radiative cooling is obtained; in this case a body could be toasted more or less evenly on all sides.

Because of the difficulties of spin stabilization one of the most promising considerations in conjunction with the design of adequate stability and damping into slender reentry bodies having high terminal velocities involves the use of flares. It has been shown by rocket-propelled-model tests conducted at the Langley Pilotless Aircraft Research Station at Wallops Island, Va., that heating loads obtained on the flared portion of blunt bodies are not unreasonable. The location of the flare at the end of the body is advantageous from the standpoint of damping because lifting elements generally contribute to pitch damping in proportion to the squares of their lever arms and lift is not generated by expanding portions of the body in front of the center of gravity which tend to cancel the contributions to stability of the rearward portions.

Work by Becker and Korycinski (ref. 3) has shown a tendency for slender flared bodies to develop large regions of separated flow in front of the flare for low Reynolds numbers at Mach numbers near 7.0. The net effect of this phenomenon is to reduce the efficiency of the flare in contributing to directional stability. This reduction in efficiency necessitates a greater area of flare than might be anticipated otherwise.

A measure of the pitch damping of two of these rocket-propelled models from a program conducted by John C. McFall, Jr., together with data from tests of a flared rounded-nose model at Thompson Aeroballistics Laboratory, is given in figure 12. These data are referenced to frontal body diameter and area rather than to base diameter and area. Adequate pitch damping is shown for all of the models in the supersonic region, but definite unstable values exist for the flared and the blunt cylinder models in the subsonic region. Similar results have been obtained at subsonic Mach numbers for a flared blunt model in wind-tunnel tests at the Langley Laboratory. Rocket-propelled-model tests on simple  $10^\circ$  cone models have indicated good damping at Mach numbers of approximately 6.0.

In one rocket-propelled-model flight, a  $10^\circ$  amplitude wandering motion of a flared model was obtained in the transonic region. Figure 13 shows the time history in this particular flight of the flared model compared with a time history for a more stable configuration. At least one wind-tunnel measurement has indicated that this flared configuration has unstable damping in the subsonic region. It is quite possible, of course, that the sharp corner is an undesirable feature of the flared configuration with regard to damping.

#### CONCLUDING REMARKS

With proper allowance for desirable geometrical features, the attainment of satisfactory stability of reentry bodies with subsonic terminal velocities is not too difficult but in efforts to minimize weight in solution of the heating problem undesirable features, such as, extremely flat noses, short skirts, and bulging afterbodies, may be incorporated into the system. Use of these features will require a much more precise determination of stability because they may produce marginal characteristics. The attainment of satisfactory stability of reentry bodies with supersonic terminal velocities appears to offer fewer problems but a number of good measurements of pitch damping are needed for low drag shapes.

Langley Aeronautical Laboratory,  
National Advisory Committee for Aeronautics,  
Langley Field, Va., March 18, 1958.

#### REFERENCES

1. Allen, H. Julian: Motion of a Ballistic Missile Angularly Misaligned With the Flight Path Upon Entering the Atmosphere and Its Effect Upon Aerodynamic Heating, Aerodynamic Loads, and Miss Distance. NACA TN 4048, 1957.
2. Faget, Maxime A., Garland, Benjamine J., and Buglia, James J.: Preliminary Studies of Manned Satellites - Wingless Configuration: Nonlifting. NACA RM L58E07a, 1958.
3. Becker, John V., and Korycinski, Peter F.: Heat Transfer and Pressure Distribution at a Mach Number of 6.8 on Bodies With Conical Flares and Extensive Flow Separation. NACA RM L56F22, 1956.

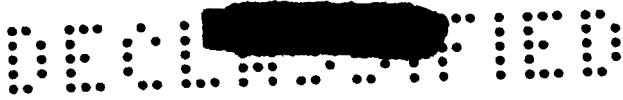
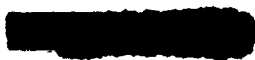


TABLE I

CONDITIONS FOR MOTION CALCULATIONS

|                      | $\frac{W}{C_D A}$ ,<br>LB/SQFT | $C_D$                                      | $C_{m\alpha}$ | $C_{N\alpha}$ | $C_{mq} +$<br>$C_{m\dot{\alpha}}$   | SPIN,<br>RPM | $I_Y$ ,<br>SLUG-<br>FT <sup>2</sup> | $\gamma$ ,<br>DEG |
|----------------------|--------------------------------|--|---------------|---------------|-------------------------------------|--------------|-------------------------------------|-------------------|
| AFTERBODY<br>SHAPE   | 113                            | 1.05 M>1<br>.70 M<1<br>1.05 M>1<br>.90 M<1 | -2            | .89           | .2 M>1<br>.1 M<1<br>0 M>1<br>.2 M<1 | 0            | 230                                 | -22 $\frac{1}{2}$ |
| TRANSONIC<br>DAMPING | 108                            | 1.11                                       | -36           | .89           | VARIES                              | 0            | 230                                 | -22 $\frac{1}{2}$ |
| SATELLITE<br>REENTRY | 29                             | 1.55 M>1<br>.90 M<1                        | -2            | .28           | 0.04 M>1<br>-.08 M<1                | 0            | 340                                 | -3                |





EFFECT OF BODY SHAPE ON PITCH DAMPING  
 $\alpha = 0^\circ$

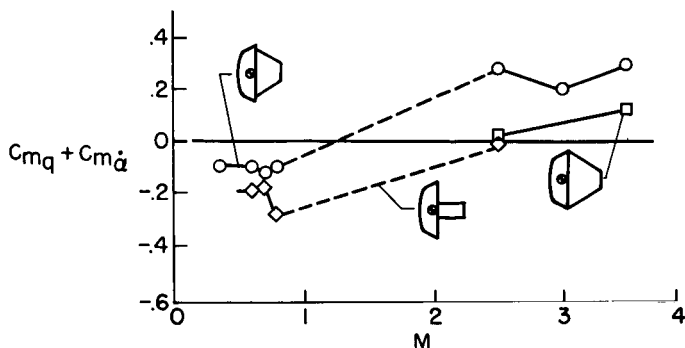


Figure 1

EFFECT OF BODY SHAPE ON PITCH DAMPING  
 $\alpha = 0^\circ$

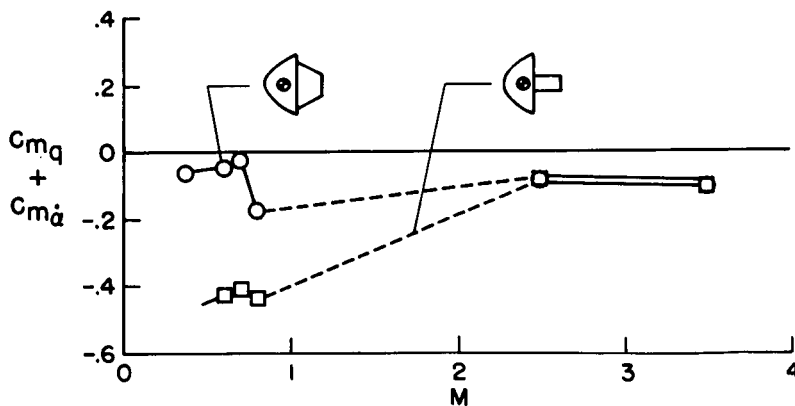


Figure 2





EFFECT OF ANGLE OF ATTACK ON PITCH DAMPING  
M=2.5

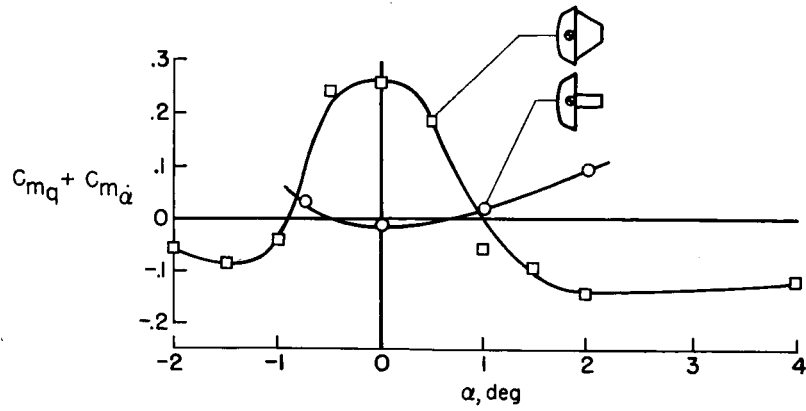


Figure 3

EFFECT OF PITCH DAMPING ON AMPLITUDE ENVELOPE  
W/C<sub>D</sub>A = 108 LB/SQ FT

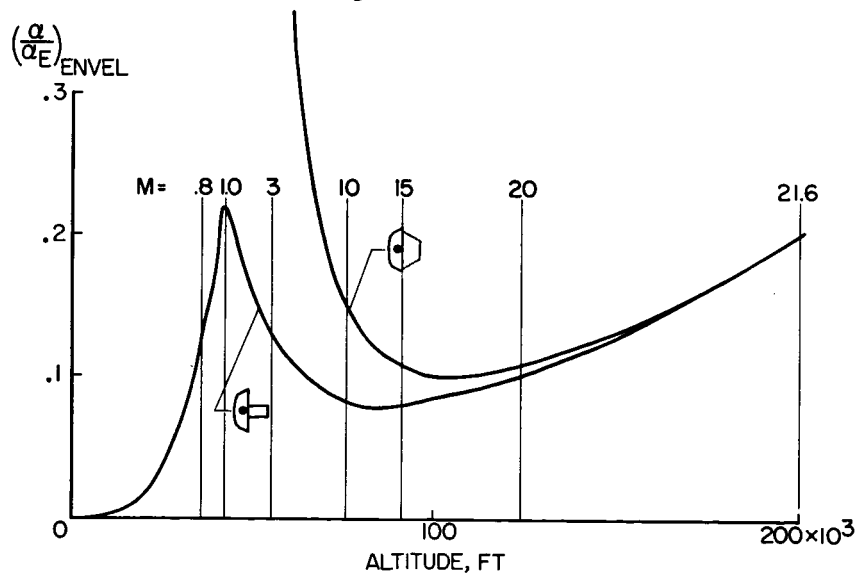
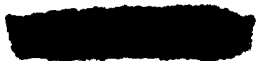


Figure 4



EFFECT OF CONTRACTION NEAR CENTER OF BODY  
 $M=1; R=5.6 \times 10^6$

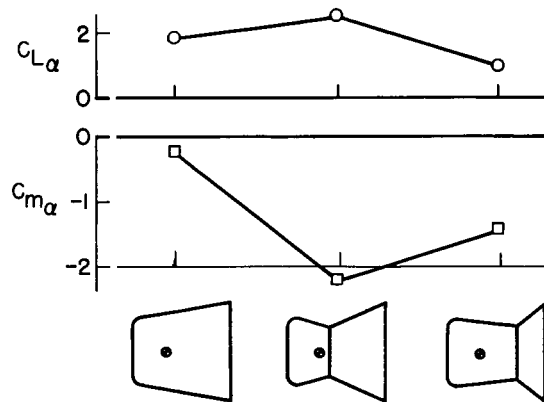


Figure 5

EFFECT OF CONTRACTION NEAR CENTER OF BODY  
 $M=3; R=6 \times 10^6$

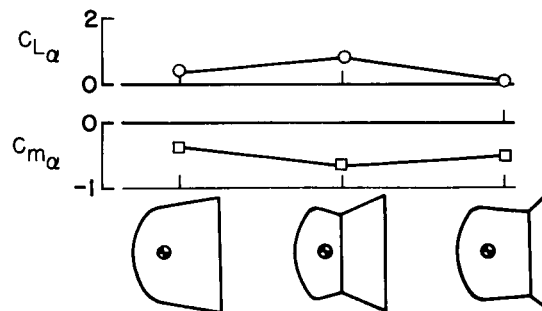
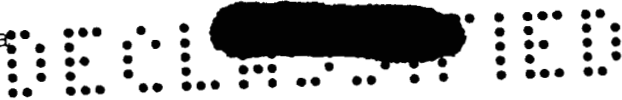


Figure 6





EFFECT OF CONTRACTION NEAR CENTER OF BODY ON PITCH DAMPING  
 $R = .65 \times 10^6$

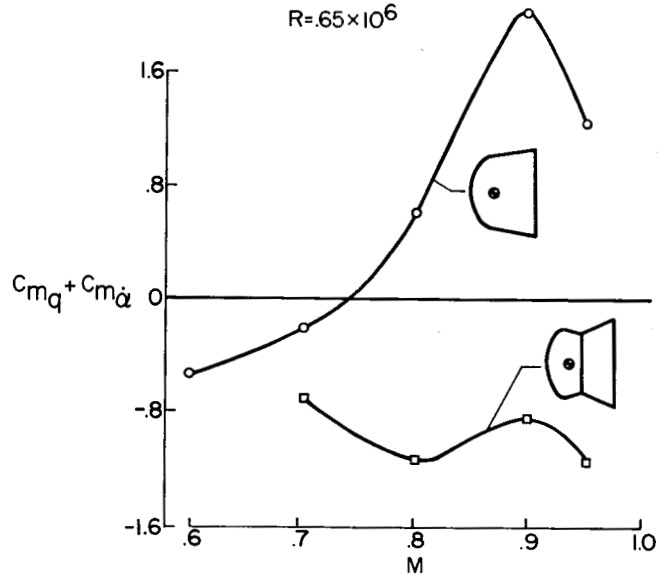


Figure 7

EFFECT OF UNFAVORABLE DAMPING IN TRANSONIC REGION

$$\frac{W}{C_D A} = 108 \text{ LB/SQ FT}$$

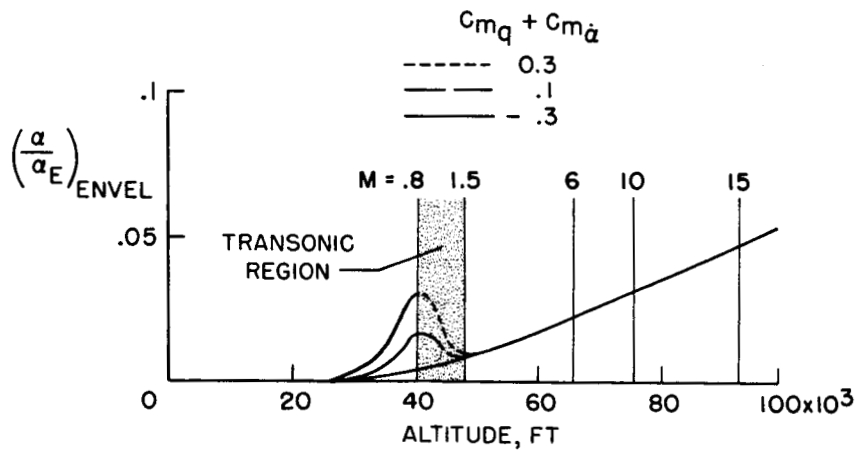
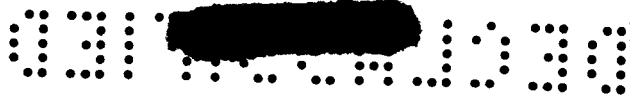


Figure 8





MOTION OF BALLISTIC REENTRY CAPSULE

$\gamma = -3^\circ$  AT 400,000 FT;  $\alpha_E = 1^\circ$

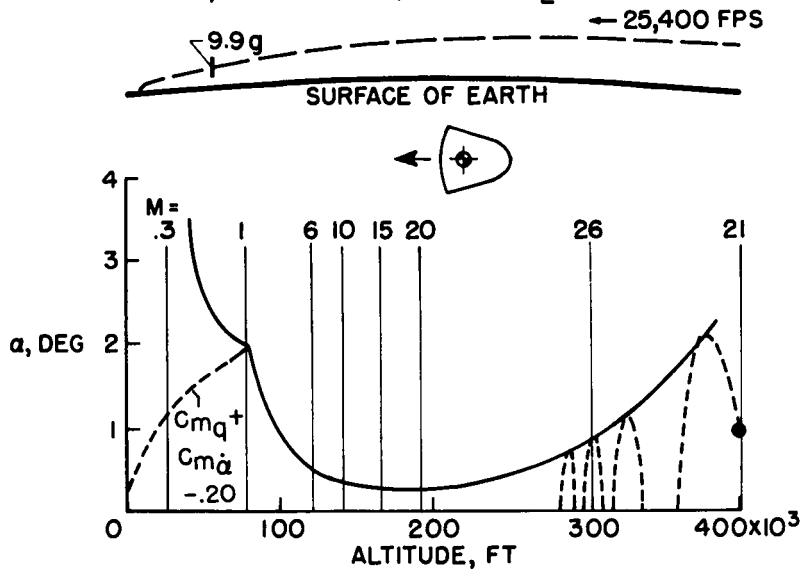


Figure 9

MOTION OF BALLISTIC REENTRY CAPSULE

$\gamma = -3^\circ$  AT 400,000 FT;  $\alpha_E = 1^\circ$

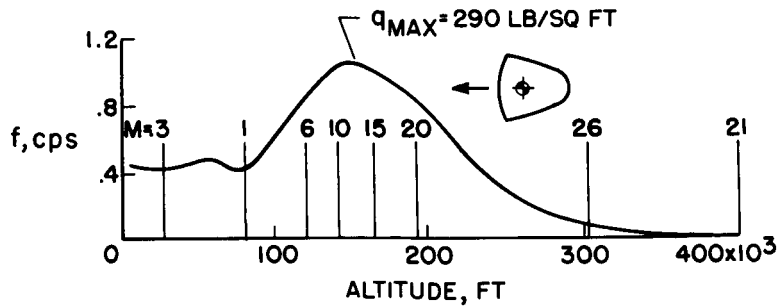
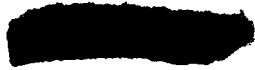


Figure 10



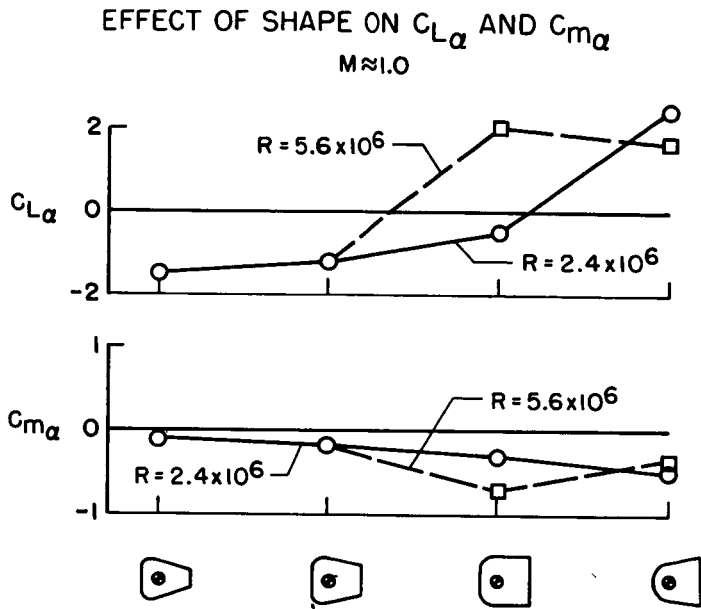


Figure 11

PITCH DAMPING OF HIGHER FINENESS RATIO MODELS

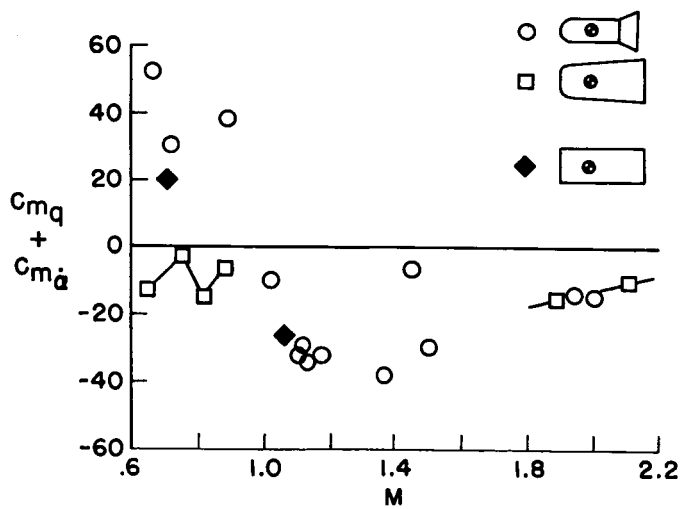


Figure 12



MOTION OF ROCKET-PROPELLED MODELS  
M=1.4

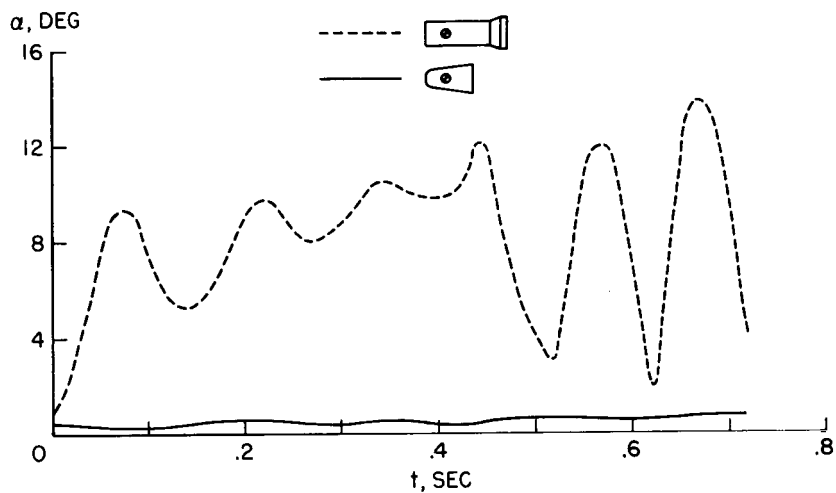


Figure 13

